

mesons were given a large amount of energy in the initial event they would decay almost immediately and produce a pair of  $\gamma$ -rays, which would then create the electron shower. Recent calculations by Heitler and Power<sup>33</sup> indicate that "transverse" mesons of short lifetime may be responsible for the production of electron showers.

Whatever the actual mechanism for production of high energy electrons may be, it seems clear that they are produced simultaneously with penetrating particles and may absorb enough

<sup>33</sup> W. Heitler and S. Power, *Phys. Rev.* **72**, 266 (1947).

of the primary energy to account for the very energetic electron air showers observed by Auger and others. It seems likely that primary particles and possibly high energy neutrons created by them are responsible for the showers observed. The frequency of events observed is not inconsistent with the number of primaries expected at sea level as estimated from the somewhat uncertain values of primary intensity and absorption in the atmosphere.

I am indebted to Professor R. B. Brode for his friendly interest in this experiment and to Professor J. R. Oppenheimer and Professor W. E. Hazen for stimulating discussions.

## Energy Distribution of Photoelectrons from Polycrystalline Tungsten\*

L. APKER, E. TAFT, AND J. DICKEY

*General Electric Research Laboratory, Schenectady, New York*

(Received September 19, 1947)

Total-energy distributions of the photoelectrons from aged polycrystalline tungsten ribbons, with the usual rolling texture, were determined by applying retarding potentials to spherical collectors. Particular attention was paid to the region of low energy. When stray fields were eliminated, energy-distribution functions rose linearly with energy. The average work function was determined by extrapolation of (current)<sup>1</sup>-voltage curves to the saturation line. The result agreed with the value 4.49 eV determined both from the spectral distribution and from the temperature variation of the photo-current. Application of spherical photo-cells to investigations of semiconductors is discussed briefly.

### 1. INTRODUCTION

USING simple assumptions about photoelectric emission from a Sommerfeld metal, Fowler<sup>1</sup> and DuBridge<sup>2</sup> developed graphical methods for analyzing photoelectric data. These techniques are convenient for determining the work functions of metals used as reference surfaces in studies of semiconductors.<sup>3</sup> This paper reports work done in preparation for such investigations.

The general theory of the photoelectric effect<sup>4</sup> has justified the assumptions of Fowler and DuBridge for a uniform, ideal metal surface with a potential barrier rounded by an image field. Faces of metallic single crystals approximate this ideal case. For such surfaces, Fowler's work provides a simple interpretation of the spectral distribution near the threshold. DuBridge's analysis treats the temperature variation of the photo-current and the energy distribution of the emitted electrons.

These techniques had their original success, however, when applied to polycrystalline metals.

\* Presented in part at the meeting of the American Physical Society, New York, New York, January, 1947.

<sup>1</sup> R. H. Fowler, *Phys. Rev.* **38**, 45 (1931).

<sup>2</sup> L. A. DuBridge, *Phys. Rev.* **39**, 108 (1932); **43**, 727 (1933); *New Theories of the Photoelectric Effect* (Hermann and Cie, Paris, 1935).

<sup>3</sup> R. A. Millikan, *Phys. Rev.* **18**, 236 (1921); E. U. Condon, *Phys. Rev.* **54**, 1089 (1938).

<sup>4</sup> K. Mitchell, *Proc. Camb. Phil. Soc.* **31**, 416 (1935); L. I. Schiff and L. H. Thomas, *Phys. Rev.* **47**, 860 (1935); R. D. Myers, *Phys. Rev.* **49**, 938 (1936); A. G. Hill, *Phys. Rev.* **53**, 184 (1938); R. E. B. Makinson, *Proc. Roy. Soc.* **A162**, 367 (1937); H. Y. Fan, *Phys. Rev.* **68**, 43 (1945).

In such cases, work functions may vary from point to point by several tenths of a volt. Empirical values are more or less complicated averages, the exact magnitudes of which depend on the particular methods of determination. Simple interpretations of such results may give rise to discrepancies, as careful investigations in thermionics have shown so clearly in the past ten years.<sup>5</sup>

The work reported here was done to test the agreement of three useful photoelectric methods in determining the "average work function" of polycrystalline ribbons. The spectral distribution of the photoelectric yield was analyzed by Fowler's method. The temperature variation of the yield was treated by DuBridge's method. Current-voltage data were compared with DuBridge's analysis of the total-energy distribution of the photoelectrons, and the work function was determined from the emission energies. Particular attention was given the region of low energies, in which results for other materials do not agree.<sup>6</sup>

Work functions determined by the three methods agreed to within a few hundredths of a volt. Fowler plots gave the value 4.49 eV. The energy-distribution function rose linearly with energy at low energies.

The new features of the photo-cells are described in Section 2. The results are given in Section 3 and are discussed in Section 4.

## 2. EXPERIMENTAL DETAILS

Figure 1 shows the construction of the two photo-cells used. They were like those previously used by Roehr,<sup>7</sup> except that the emitter supports were covered with nickel sleeves. These sleeves were held at various potentials with respect to the tungsten-ribbon emitters. Unavoidable contact-potential differences between the emitter and the supports were thus compensated.

The emitters were 99.9+ percent pure tungsten ribbons, 0.25 cm wide, 2.5 cm long, and 0.0025 cm thick. The aging treatment after assembly of the photo-cells was such that the original rolling texture was almost, but not quite, preserved. Most of the crystallites were oriented

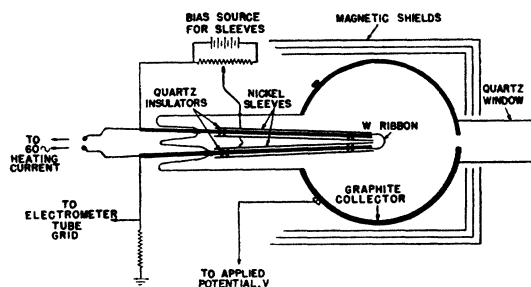


FIG. 1. Schematic diagram of photo-cell.

with (100) directions within  $10^\circ$  of the perpendicular to the ribbon surface.<sup>8,9</sup> The average crystal diameter was about 0.005 cm. At the grain boundaries there were barely detectable grooves, apparently due to preferential thermal etching. The rest of the surface appeared smooth when magnified 500 diameters.

Pressure in the tube after the seal-off was  $2.10^{-8}$  mm Hg as indicated by an ionization gauge calibrated for air.<sup>10</sup> The active gas pressure was such that the work function of the clean ribbon increased by about 0.5 eV to an equilibrium value in 4 days. The transient pressure increase caused by flashing the ribbon showed that there was roughly 20 percent of a monolayer of adsorbed gas on the contaminated tungsten. Most of this could be removed by a 10-sec. flash at  $1100^\circ\text{K}$ ; the remainder came off at  $2100^\circ\text{K}$ . Before each photoelectric measurement, the ribbon was flashed at  $2900^\circ\text{K}$ . Spectral data could be taken in 20 seconds, current-voltage curves in three minutes.<sup>11</sup>

Radiation sources for energy measurements were low pressure Zn, Cd, or Hg discharges in rare gas. The desired spectral lines were isolated with a Bausch and Lomb quartz monochromator.<sup>12</sup> No background radiation could be detected

<sup>8</sup> W. G. Burgers and J. J. A. Ploos van Amstel, *Physica* **3**, 1064 (1936); J. F. H. Custers and J. C. Riemersma, *Physica* **12**, 195 (1946).

<sup>9</sup> Mr. Eric Asp kindly took x-ray diffraction photographs of the ribbons.

<sup>10</sup> For the type of evacuation schedule used, see W. B. Nottingham, *Phys. Rev.* **55**, 203 (1939); *J. App. Phys.* **8**, 762 (1939).

<sup>11</sup> The initial contamination rate after a flash caused the saturation photo-current for  $h\nu = 4.89$  eV to decrease by 0.1 to 0.4 percent per min. When necessary, plots of current vs. time were extrapolated back to the time zero. No effects due to contamination were found. See C. E. Mendenhall and C. F. DeVoe, *Phys. Rev.* **51**, 346 (1937).

<sup>12</sup> We are indebted to the University of Rochester Physics Department for the loan of this instrument.

<sup>5</sup> M. H. Nichols, *Phys. Rev.* **57**, 297 (1940); **59**, 944A (1941); W. B. Nottingham, *Bull. Am. Phys. Soc.* **22**, 14 (1947).

<sup>6</sup> E. Rudberg, *Phys. Rev.* **48**, 811 (1935). For a discussion, see A. G. Hill, *Phys. Rev.* **53**, 184 (1938).

<sup>7</sup> W. W. Roehr, *Phys. Rev.* **44**, 866 (1933).

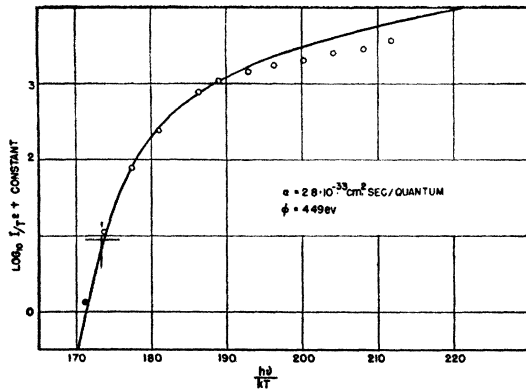


FIG. 2. Fowler plot for normal incidence and for  $T = 300^\circ\text{K}$ . The point at the extreme left is an upper limit set by the sensitivities of the thermocouple and the current detector. For currents measured in electrons/quantum, the additive constant on the ordinate scale is  $-7.765$ .

between lines. Intensities were constant to 0.2 percent. On the emitter, the area illuminated varied from 0.5 to 1.0 mm<sup>2</sup>. The angle of incidence could be changed by moving this spot over the surface. For spectral measurements, Hg arcs operating at 2 atmospheres served as sources. In this case, intensities were constant to 1 percent, and corrections for background were made when necessary.

Intensities were determined with a compensated vacuum thermocouple<sup>13</sup> calibrated against a standard radiation source from the Bureau of Standards. Currents were measured with a split FP-54 electrometer tube<sup>14</sup> using a  $5 \cdot 10^{10}\Omega$  grid resistor and a sensitivity of 50,000 mm/volt.

### 3. RESULTS

Figure 2 is a Fowler plot for the clean ribbon. The parameter  $\alpha$  in Fowler's equation,  $I = \alpha AT^2 \bar{\phi}(h\nu/kT)$ , rose from  $2.8 \cdot 10^{-33}$  cm<sup>2</sup> sec./quantum at  $\theta = 0^\circ$  to  $14 \cdot 10^{-33}$  cm<sup>2</sup> sec./quantum at  $\theta = 45^\circ$ , where  $\theta$  is the angle of incidence of the radiation. The variation was roughly parabolic near  $\theta = 0$ . The work function determined was  $\phi = 4.49 \pm 0.02$  eV.<sup>15</sup>

<sup>13</sup> Kindly made for us by Dr. C. H. Cartwright.

<sup>14</sup> J. M. Lafferty and K. H. Kingdon, J. App. Phys. 17, 894 (1946).

<sup>15</sup> The data of Fig. 2 fall below the Fowler curve for  $h\nu/kT > 190$ . This is difficult to understand, since a non-uniform surface should produce deviations in the other direction. This discrepancy, however, has no important effect on the value of the work function determined from the Fowler plot. Mendenhall and DeVoe<sup>11</sup> found that data for the faces of a single tungsten crystal fitted Fowler plots

In Fig. 3 are DuBridge isochromatic plots showing the temperature variation of the photoelectric yield for  $h\nu = 4.42, 4.49,$  and  $4.59$  eV. The temperature was changed from  $300^\circ\text{K}$  to  $1040^\circ\text{K}$ , the latter value being determined with an optical pyrometer. The work function determined was  $\phi = 4.49 \pm 0.02$  eV. Values of  $\alpha$  varied by a factor of 2.

Figure 4 shows the interesting portions of current-voltage curves for  $h\nu = 4.89$  and  $5.80$  eV. Data were taken in the range  $-10 < V < 180$  volts. Ordinates in Fig. 4 are normalized at  $V = +10$  volts. The dashed curves show the effects of the sleeve potentials. The work function of the sleeves as determined from photoelectric measurements was 5 volts. The resultant 0.5-volt contact-potential difference between the sleeves and the ribbon was thus compensated by a  $+0.5$ -volt sleeve potential. Reverse currents were present for  $h\nu = 5.80$  volts. Corrections were made by extrapolation of the reverse current line in the usual way.<sup>16</sup> This was checked by repeating the process with the ribbon contaminated, in which

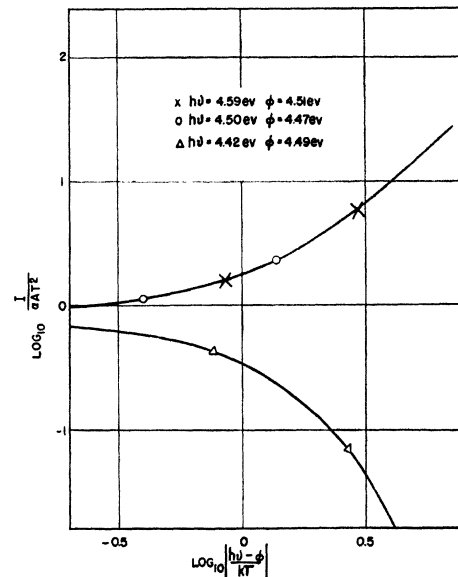


FIG. 3. Typical DuBridge plot for the temperature variation of the photoelectric yield between  $300^\circ\text{K}$  and  $1040^\circ\text{K}$ . For each value of  $h\nu$ , the corresponding value found for  $\phi$  is shown.

for a range of  $h\nu/kT$  equal to 40 when the surfaces were clean.

<sup>16</sup> P. Lukirsky and S. Prilezaev, Zeits. f. Physik 49, 236 (1928); S. Prilezaev, J. Tech. Phys. U.S.S.R. 9, 1439 (1939).

case the reverse current was a larger fraction of the total.

Figure 5 shows a DuBridge plot for  $T=300^\circ\text{K}$  and  $h\nu=4.89$  ev. Values of  $eV_0=h\nu-\varphi_c$ , where  $\varphi_c$  is the work function of the collector, could be determined from these plots to within  $\pm 0.01$  volt. Points so determined are marked with arrows in Fig. 4.

Figure 6 shows the current-voltage curves plotted on a parabolic scale. Currents were normalized at  $V=+0.7$  volt, a point definitely on the saturation line. The plots were insensitive to the particular value of  $V$  selected for normalization. Saturation points determined by this extrapolation process were  $V_s=+0.62\pm 0.02$  volt. The extreme range of these values is shown by the brackets above the arrows in Figs. 4 and 6. The value of  $\varphi$  determined from Einstein's relation,  $\varphi=h\nu-e(V_s-V_0)$ , was  $4.48\pm 0.03$  ev.

The saturation lines in Fig. 4 were clearly not horizontal. Between  $V=10$  and  $V=180$  volts the photo-current increased 4.5 percent for

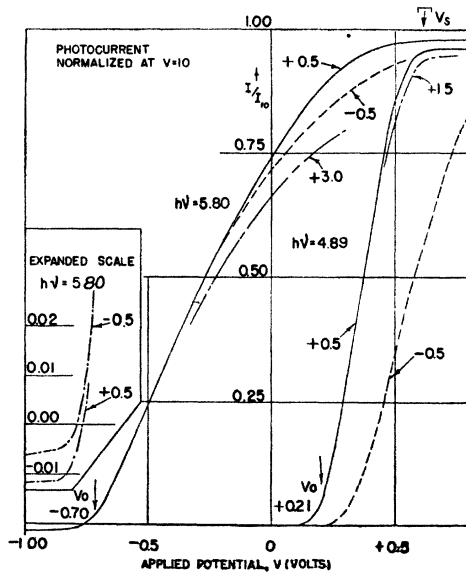


FIG. 4. Portions of typical current-voltage curves for  $h\nu=4.89$  and  $5.80$  ev;  $T=300^\circ\text{K}$ . Complete curves extended from  $V=-10$  to  $+180$  volts. The photo-current at  $V=+10$  is set equal to 1. The ordinates for  $h\nu=5.80$  ev are expanded by a factor of ten in the inset to show the behavior of the exponential temperature "tails" in the presence of reverse currents. Sleeve potentials in volts are written next to the curves; a value of  $+0.5$  compensates for the effect of stray fields. Experimental points were taken at intervals of  $0.02$  volt near the tails and near the saturation points. Their deviation from the curves is not visible on this scale. Arrows mark the values of  $V_0$  and  $V_s$  determined from Figs. 5 and 6, respectively.

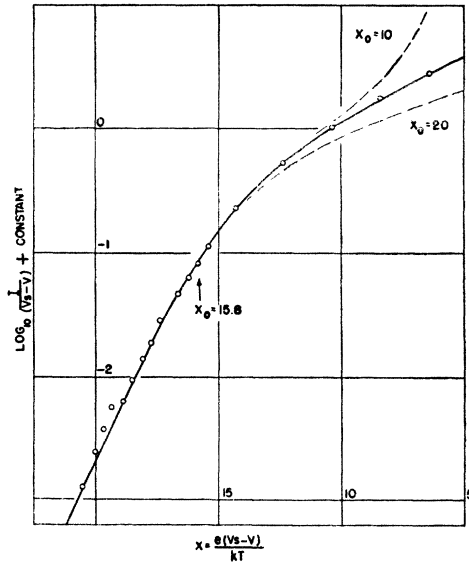


FIG. 5. Typical DuBridge plot for total-energy distribution.  $T=300^\circ\text{K}$ ;  $h\nu=4.89$  ev. The theoretical curve for  $x_0=(h\nu-\varphi)/kT=15.8$  is shown as a solid line; curves for  $x_0=10$  and  $20$  are dashed. The value of  $V_0$  determined from this plot is  $+0.21$  volts. It shows a negligible dependence on the value of  $V_s$  used in evaluating  $x$ . In this case,  $V_s=+0.62$  volt was taken from Fig. 6.

$h\nu=4.89$  ev and 1.8 percent for  $h\nu=5.80$  ev. From the geometry, rough estimates were made of the field  $F$  at the emitting area.<sup>17</sup> Plots of  $I$  vs.  $F^{\frac{1}{2}}$  had roughly 5 times greater slope at  $F=1$ -volt  $\text{cm}^{-1}$  than that calculated from Fowler's equation and Schottky's relation,  $\Delta\varphi=(eF)^{\frac{1}{2}}$ ; at  $F=100$ -volt  $\text{cm}^{-1}$  the experimental slope was less than 2 times the theoretical value.

#### 4. DISCUSSION

The results in Section 3 show that the methods of Fowler and DuBridge gave consistent values for the work function of two polycrystalline tungsten ribbons. The slopes of the saturation lines in Fig. 4 indicate that there were surface non-uniformities with a patch spacing larger than those normally found in thermionic work.<sup>18</sup> The three methods used for determining work functions represent quite different kinds of averaging over these patches, but the results differed by only a few hundredths of a volt. A similar result

<sup>17</sup> We are indebted to Mr. R. N. Hall for the results of his calculation of the field in a spherical condenser with a radial support.

<sup>18</sup> J. A. Becker, Rev. Mod. Phys. 7, 95 (1935); C. Herring, private communication.

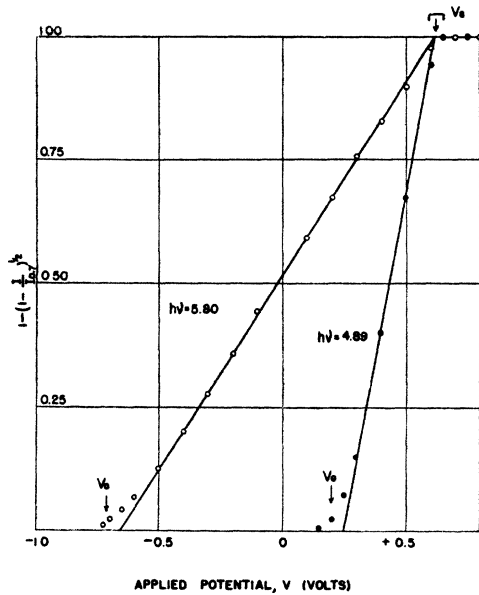


FIG. 6. Current-voltage data for  $h\nu = 4.89$  and  $5.80$  eV plotted on a parabolic scale. The extreme range over which  $V_s$  varied for six sets of data is shown by the bracket over the upper arrow. The lower arrows show values of  $V_0$  determined from Fig. 5. DuBridge's analysis gives a straight line passing through  $V_0$  and  $V_s$  at  $0^\circ\text{K}$ .

has been obtained in early work on the equality of the photoelectric and thermionic work functions for other metals.<sup>2,19</sup> An emitter with a small fraction of its area occupied by patches of higher work function than the rest would behave in this manner. It is of interest in this connection that the average work function of the tungsten ribbons used here is close to Nichol's value of 4.56 eV for the thermionic work function associated with the (100) direction in single-crystal tungsten wire.<sup>5,20</sup>

In the low energy region, the current-voltage

<sup>19</sup> Interpretation of such comparisons is complicated by the wide difference between the temperatures at which photoelectric and thermionic phenomena are observed. For discussions see F. Seitz, *The Modern Theory of Solids* (McGraw-Hill Book Company, Inc., New York, 1940); C. Herring *Phys. Rev.* **59**, 879 (1941).

<sup>20</sup> Dr. Nichols has kindly informed us that his published value, 4.53 eV, is 0.03 eV too low because of a computational error.

characteristics of Fig. 4 are parabolic, corresponding to a total-energy distribution function rising linearly with energy. This point has been the subject of previous discussion.<sup>2,6,21</sup> Henshaw has obtained an analogous result in work on the normal-energy distribution of photoelectrons from potassium films.<sup>22</sup>

The surface properties of semiconductors can be investigated with particular convenience in spherical photo-cells with interchangeable emitters.<sup>3</sup> Work functions of metals used for purposes of comparison can be found by the methods of Fowler and DuBridge, but for semiconductors this is not the case. Prilezaev in work on  $\text{SbCs}_3$ , a non-metallic material, has used the saturation point of current-voltage curves to determine contact-potential differences.<sup>16</sup> Since the collector work function was known, the emitter work function could be obtained. The results in Section 3 show that this procedure is sensitive to stray fields. Where these are compensated, however, work functions so determined for tungsten agree with those found by the two other methods used.

Current-voltage curves for metallic emitters fall to zero exponentially when  $V$  is of the order of 0.1 volt more negative than  $V_0 = (h\nu - \varphi_c)/e$ . For ideal semiconductors they approach zero in a different way at values of  $V$  several tenths of a volt more positive. Inspection of Fig. 4 shows that such an effect is also found for metals if stray retarding fields are present. The region near the saturation point is even more easily distorted. Retarding-potential measurements, especially at low energies, are obviously not reliable unless these fields are eliminated.

#### ACKNOWLEDGMENTS

We are indebted to Dr. C. Herring and Dr. J. A. Burton for helpful discussions of this work.

Dr. A. W. Hull has given us the benefit of his interest and advice.

<sup>21</sup> I. Liben, *Phys. Rev.* **51**, 642 (1937).

<sup>22</sup> C. L. Henshaw, *Phys. Rev.* **52**, 854 (1937).